Case Studies in Thermal Engineering 74 (2025) 106755

Contents lists available at ScienceDirect

Case Studies in Thermal Engineering

journal homepage: www.elsevier.com/locate/csite

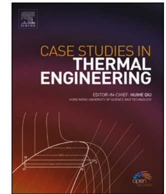

Three-dimensional nano-structure investigation on a thermo- and electrical conductive adhesive via X-ray imaging

Minghao Yin [a,b,1], Dadong Wang [c,1], Yan Zhong [c], Ian Robinson [d], Bo Chen [a,d,*]

[a] *Key Laboratory of Advanced Civil Engineering Materials of the Ministry of Education, School of Materials Science and Engineering, Tongji University, Shanghai, 201804, China*
[b] *School of Materials and Chemistry, University of Shanghai for Science and Technology, Shanghai, 200093, China*
[c] *Shanghai Highway Investment Construction and Development Co., Ltd., Shanghai, 200336, China*
[d] *London Centre for Nanotechnology, University College London, London, WC1H 0AH, UK*

GRAPHICAL ABSTRACT

Nano-structure of the silver conductive adhesive.

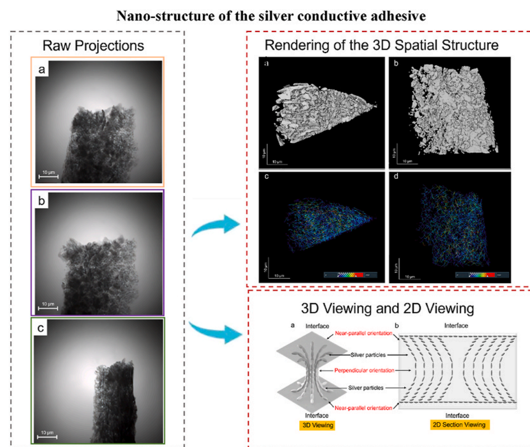

ARTICLE INFO

Keywords:
Silver particles
Epoxy adhesive

ABSTRACT

Nowadays, advancements in adhesion of huge amount of electronic components have evolved from using traditional soldering to conductive adhesives, notably silver-based ones, offering cost

* Corresponding author. Key Laboratory of Advanced Civil Engineering Materials of the Ministry of Education, School of Materials Science and Engineering, Tongji University, Shanghai, 201804, China.
E-mail address: bo.chen@tongji.edu.cn (B. Chen).

[1] These authors contributed equally to this work.

https://doi.org/10.1016/j.csite.2025.106755
Received 13 February 2025; Received in revised form 1 July 2025; Accepted 24 July 2025
Available online 26 July 2025
2214-157X/© 2025 The Authors. Published by Elsevier Ltd. This is an open access article under the CC BY-NC license (http://creativecommons.org/licenses/by-nc/4.0/).

Continuum conductive paths
Thermal conductivity
X-ray microscopy

efficiency, health safety, and superior thermal conductivity, which is crucial for the increasing computational speeds and thermal management in microelectronics. Hence it is imperative to undertake a comprehensive analysis of these materials. In this work, the inner structure of a silver adhesive applied in splicing electronic components was investigated to reveal the mechanisms and factors of its thermal and electrical conductance. Transmission X-ray microscopy (TXM) with nanoscale resolution (for three-dimensional (3D) imaging) was used to characterize the samples. The results demonstrate that the regularly concentrated silver particles, mostly with a length less than 1 μm and with a volume less than 1 μm^3 with flaky shape, are arranged to form the continuum conductive paths inside the matrix materials. The thermal and electrical conductance of this adhesive have been studied and analyzed, and proven to be superior along the surface-normal direction. The nearly-perpendicular grain orientation of the inner silver particles and the parallel orientation of the particles next to the adhesive surfaces both act to optimize the conductance of the heat and electrons of this materials.

1. Introduction

Since 1980, research and development of the conductive adhesives was credited with saving the production costs of a large number of electronic products. In addition, conductive adhesives could reduce the health hazards associated with conventional lead-tin solder technology, which is a significant advantage [1]. With the continuing advancement of microelectronics, there is a fast growing interest in advanced adhesive materials with excellent thermal conductivity. This is due to a second important issue, namely thermal radiation, which is unavoidably connected with the ever-increasing speed of computation and processing of microelectronics, especially for the coming artificial intelligence (AI) era. Thermal radiation can directly affect the lifetime and efficiency of the electronics. An increase in temperature by 10–15°C could result in halving the device life [2]. Therefore, materials are urgently needed for fast thermal conductivity to protect electronic devices [3–5]. Among them, silver-based electrically conductive adhesives (ECAs) have gained widespread use. Compared with other types of adhesives, silver-based ECAs have many advantages such as lower toxicity, fewer processing steps, excellent thermal conductivity and excellent stability to various substrates. These have made silver-based ECAs a major adhesive used in electronic products such as liquid crystal displays, light-emitting diodes, integrated circuit chips, and radio frequency identification tag antennas [6–8].

In general, silver-based ECAs consist mainly of two components: a polymer matrix (such as epoxy) and a conductive filler (i.e. silver particles), providing the mechanical strength and the desired conductivity, respectively. Commonly-used conductive fillers are nano/micro-sized silver with granular, flake, ribbon, and wire shapes. To improve the thermal conductivity of epoxy resin adhesives, highly conductive fillers, such as graphene nano-sheets and MXene fillers, are also incorporated into the epoxy matrix to enhance its heat dissipation capabilities [9–12]. The superior thermal conductivity of silver-based ECAs can be originated from the primary heat carriers in the materials, i.e. electrons and phonons [13–15]. Hence, the addition of fillers with very high thermal conductivity such as silver metals into polymer based adhesives becomes the main method to improve their thermal conductivity. They form a thermally conductive network that facilitates rapid heat transfer, thereby enhancing the adhesive's thermal conductivity.

In recent years, to optimize the network structures of the conductive fillers, lots of investigations have been focused on improving the size of the silver particle fillers or using synthetic composites such as functional graphene materials with silver-containing particles as fillers [16,17]. Other studies have proposed nanowire structures for thermally conductive silver adhesives, which can enhance both the thermal conductivity and mechanical properties of the silver adhesives through the high specific surface area and unique electronic structure of nanowires [18]. In addition, some researchers have sought to enhance the thermal conductivity and stability of the silver adhesives by introducing organic and inorganic hybrid structures [19,20]. Zulkarnain et al. studied the influence of the ratio of silver particles to silver nanoparticles on their thermal conductivity [21]. Li et al. prepared a three-dimensional (3D) silver-filled structure of ECAs using silver fractal "flowers" (Ag-FFs) as the main fillers and silver nanowires (Ag-NWs)/silver nanoflakes (Ag-NFs) groups as auxiliary fillers [22]. These ECAs prepared by constructing 3D conductive networks have good conductivity and resistance stability, and the content of silver particles needs to be moderate to balance conductivity and adhesive performance [23,24]. Although various research has been done on ECAs, the main silver fillers of most commercial adhesives available today are still in the micro-scale [25–28]. Meanwhile, conventional micro-silver filled adhesives suffer from some drawbacks, such as the silver fillers are usually produced by ball milling and covered with insulating (organic) lubricants, thus their tunnel resistance is quite high [29]. In addition, these ball milled silver sheets always with rough surface that easily lead to greater resistance which results from the point-to-point contact among this shape of particles [26]. These would reduce the thermal and electrical conductivity of the adhesives. Secondly, micron-sized silver particles would always generate more gaps, i.e. more pores in the adhesives, when they are contacted in the network thus reducing the thermal conductivity. While, nano-silver particles for filling can effectively improve this situation.

As a thermal and electrically conductive adhesive, the primary applications of the silver epoxy adhesives are attaching silicon chips to substrates or heat sinks, while also ensuring mechanical integrity [30]. In these instances, it is the thermal conductivity, not electrical conductivity, that is most crucial, as the performance of modern integrated circuits is largely determined by the efficient heat dissipation from the active semiconductor structure.

When the concentration of the silver particles in the epoxy matrix surpasses a critical threshold, a conductive path is established [31]. Right at the critical concentration, a "percolation transition" occurs, which means the conductive "paths" begin to form in the insulating matrix. With further increases in the concentration of silver particles, a richer 3D spatial network of the conductive paths

established, and the conductivity of the cured adhesive coating layer further increased until reaching a peak value and remaining nearly constant [31]. A high ratio of silver filler can be effective in achieving sufficiently high electrical conductivity. However, higher filler content also implies lower adhesion [32]. It naturally follows that the next problem is how to strike a balance between the amount of silver and epoxy used in the formulation to create a satisfactory silver epoxy adhesive having decent thermal conductivity and adhesion. The orientation of the particles on the micro- and nano-scale is highly relevant, which would refine the conductive efficiency.

Percolation theory [33,34] can be used to explain the thermal and electrical conductivity of the silver epoxy adhesive and its variation pattern with particle concentration. To apply this to understand the conductivity origin of the materials, information about the real 3D structure is needed. This study employed X-ray tomography to analyze a silver epoxy adhesive [35,36] at the nanoscale to visualize the 3D spatial network of the conductive silver particle paths within it. The sample consists of two main parts: flake-shaped silver particles and matrix epoxy resin. The silver particles, usually a few microns in size, account for about 80% of the weight of the (dried) adhesive sample. X-ray nano-tomography measurements provided detailed 3D images of the silver particles' shapes, sizes, and spatial distribution, revealing the conductive network made by these particles that provide pathways for percolation of heats and electrons within the materials [37–39], which governs its thermal and electrical properties. Our work further reveals and suggests the conductive adhesive of a structure containing the fillers with parallel orientation near surfaces and with vertical alignment within the internal body. The dedicated structure presents an approach to enhancing thermal and electrical transfer performance. This study fills the gap of correlations between the 3D spatial nano-structure of the conductive adhesives and their thermal and electrical conductivities.

2. Materials and methods

The measured samples were dry silver epoxy adhesive films that have been applied on surface-treated glass slices and been cured over a year at room temperature. The acquisition of the X-ray tomographic data and the 3D image reconstruction were performed by using a transmission X-ray microscopy (TXM), Zeiss Xradia X-ray Nano-CT (Ultra series).

Before measurement, the samples were peeled off from their substrates to become free-standing films. Then, the films were cut into smaller pieces and fixed on the tips of pins by cyanoacrylate glue. The fixed samples were then fabricated into tiny triangle-shaped samples that were then mounted in the TXM sample holders for measurements. During the tomographic measurements, the reference 2D projection images with the X-ray beam only were collected for use as the background image of the final tomographic scan data. The final tomographic scan was performed with 0.15° angular step in a scanning angular range from −90° to 90°, giving in total 1201 absorption contrast projections of the sample for the 3D reconstruction. The measurements were performed under absorption contrast (only) mode using a quasi-monochromatic X-ray source of 8.05 keV ($\lambda \approx 1.54$ Å) at 40 kV acceleration voltage from a copper rotating anode target. The field of view (FoV) of $66 \times 66\ \mu m^2$images of the samples were generated with 1024×1024 pixels which gives out the reconstructed pixel size of 64.45 nm × 64.45 nm.

3. Results and discussion

Raw X-ray projections at a series of different angles (−45°, 0° and 45°) of a free standing film sample are shown in Fig.s 1a, 1b and 1c, respectively. The size of the projections is $66 \times 66\ \mu m^2$.

As the projection images were collected in the absorption contrast mode during tomographic scan, the epoxy appears nearly transparent to the X-rays and could hardly contribute to the absorption images. Hence, in Fig. 1, the darker regions (in the middle) are the silver particles that exhibit significantly higher X-ray absorption than that of the epoxy resin.

Fig. 2 presents the tomogram slice images of the sample. Because the sheet-shaped sample was positioned vertically to the horizontal plane (i.e. parallel to the rotation axis Z), with its surface also perpendicular to the horizontal (shown in Fig. 3b as well). These tomogram slices (in Fig. 2) illustrate the sample's structure from its film surface to the film-substrate interface. Ideally, the cross-sections of the sample slices should be close to rectangle-shaped, rather than the wedge-shaped shown in these images. As the

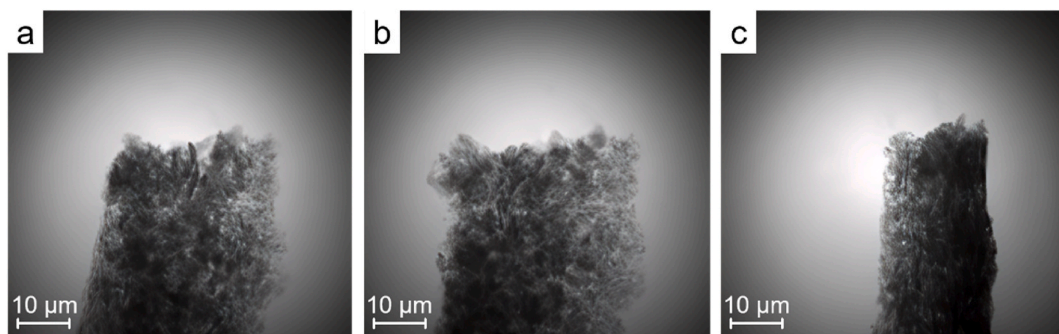

Fig. 1. A series of raw projections of the silver epoxy adhesive. (a) A projection at −45°. (b) A projection at 0°. (c) A projection at 45°.

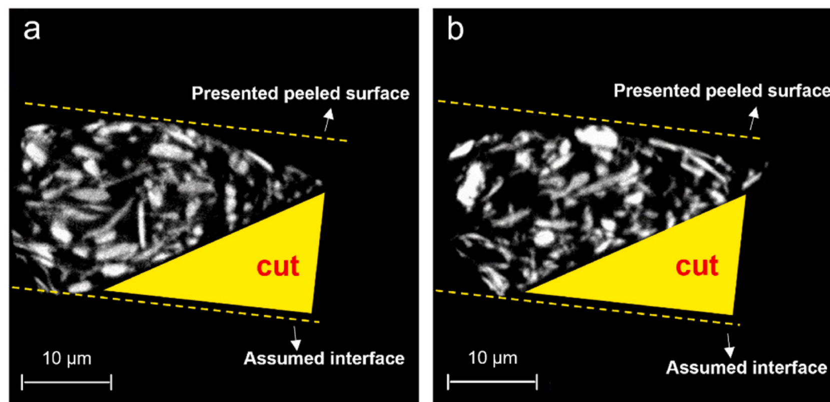

Fig. 2. The reconstructed X-ray tomogram slices of the 3D image of the silver epoxy adhesive in the zx plane (perpendicular to the tomography rotation axis Z).

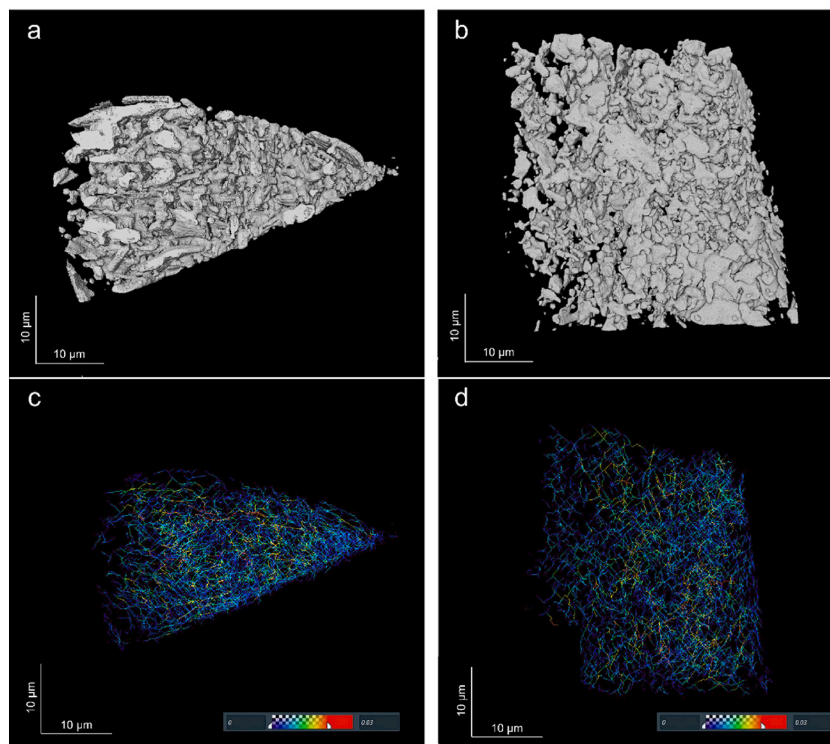

Fig. 3. 3D structural image rendering of the silver adhesive. (a) Side view of the image in xy plane (perpendicular to the rotation axis Z). (b) Side view of the image in xz plane (parallel to the rotation axis Z). (c) & (d) The simplified centerline network of the connected silver particles along the same orientations in panels a & b.

broken yellow lines indicated in Fig. 2, the (ideal) surface and interface should be parallel to each other. However, during the sample fabrication, part of the interface region was cut, and hence produced the wedge-shaped sample.

For the following 2 reasons, it was concluded that the marked higher side (in Fig. 2) is the intact peeled surface. The sample directly adheres to the substrate coated with release agent so that the peeled-off surfaces cannot be totally flat and straight because of the deformation during the peeling-off operation. In contrast, the cut side of the sample can be rationally flat because of the inertia in force direction during the cutting process, especially at the tiny scale.

Fig. 3 presents a rendering of the reconstructed 3D spatial structure of the sample, in which Fig. 3b shows the presumed peeled surface. The silver particles within the sample were rendered in silvery color (in Fig. 3). From 3D perspective, these images show that the particles have a plate-like shape, rather than the pellet-liked shape as shown in the 2D slices as well.

The preserved surface obviously shows many bulks of Ag particles in flake-shape with relatively larger area (Fig. 3b), but the other

side, i.e. the damaged cut side, is different (Fig. 3a). For the damaged side, the closer to the thicker side (Fig.s 3a & 3b) where more parts of the sample surface were conserved, the more silver bulks appear. This indicates the damaged side has lost many information which is possible in consonance with the preserved surface where many plate-shaped silver particles with large area existed. Near the preserved surface, the plate-shaped silver particles tend to align almost parallel to the surface (see the higher parts in Figs. 3a and 2).

After 3D digital image segmentation, every segmented Ag particle was labelled, and then the centerlines of the contacted labelled objects, i.e. the Ag particles, were extracted and rendered as a network (Fig.s 3c & 3d). The Euclidean distance from the points of the centerline of the labelled object to the nearest object boundary is stored as thickness of the object at each point. These values were used as an estimate of the local thickness and reflect the color brightness and thickness of the object. The rendered skeleton-like result clearly shows the connectivity with orientation distribution and the general relative thickness of the Ag particles, and the color-map of the presented skeleton is determined by the thickness of each point (Fig.s 3c & 3d). It is found that the centerlines on the higher side (of the preserved surface) are almost parallel to the surface plane, interweaving like a net structure (Fig. 3c). As to the lower side (in Fig. 3c), the centerlines orientation of its left part (partly preserved interface) is similar to the preserved surface, but the right part (cut part) is quite different, containing many lines with a vertical orientation. Moreover, the points with higher color saturation, i.e. of higher thickness, are mainly distributed near the surface. These indicate that the orientation arrangements of the silver particles are quite different among the surface parts and the inner parts, and that the larger silver particles tend to congregate near the surface along the direction parallel to the surface.

The length and volume distributions of the silver particles are presented in Fig. 4. The silver particles are divided into 11 groups by length from 1 μm to 10 μm with 2 extra groups of lengths less than 1 μm and longer than 10 μm, and they are divided into 9 groups by volumes from 1 μm^3 to 35 μm^3 with 2 extra groups of volumes less than 1 μm^3 and larger than 35 μm^3. It can be seen that more than half of the particles (63.50%) are smaller than 1 μm, with decent portion of particles of a few microns and very small amount of particles larger than 10 μm.

To further investigate the local internal structure, a representative part of a cube (Fig. 5b) which includes a part of the preserved surface was cropped from the measured sample (Fig. 5a) for study. The particle centerline network path was calculated as well. The segment color-map of the centerlines is also indicated by the thickness at each point (Fig.s 5a-5c). Within the cube, it is showing that the centerlines of the silver particles cross-contacted and their connections are generally aligning towards the surface normal. At the same time, along the surface parallel direction, the particle connections are frequently interrupted. Along the direction perpendicular to the sample surface, the occupied areas of the silver particles of each tomogram slice were measured (Fig. 5d). It is easy to understand that the rapid rise of the occupied areas from slice 0 to slice 25 which resulted from the uneven surface, whose initial slices were fragmented. Ruling out the beginning interference items (about slice 0 to slice 25), the statistical area was divided into two parts. One is from about slice 25 to about slice 100, where the average area per slice occupied by silver particles was about 1.25 μm^2. The other part is from about slice 101 to the end, where the area per slice was about 1.12 μm^2 with a slight fluctuation. The former part is closer to the surface with more parallel-oriented particles, so it has larger average area than that of the latter part. This also indicates that the orientations of the silver particles are different between the surface regions and internal regions as mentioned above.

Based on the measured structure, Fig. 6 shows a schematic model of the desired structural arrangement of the silver particles within the adhesive which could enhance its thermal and electrical conductive properties. For this structure, the adhesive films would obtain superior thermal and electrical conductivities because the (device-generated) heat and electrons can propagate directly through the cured films along the inter-connected conductive silver particles that lie perpendicular to both interfaces (at device and heat-sink sides). Meanwhile, the near-surface-normal orientation of the silver particles in the inner parts of the cured adhesive could form shorter conducting paths, which means shorter conducting distances and shorter cooling time for heat. Furthermore, the near-parallel arrangement of the silver particles close to the interfaces increases their contact area with both external interfaces, namely the semiconductor device and the heat sink. This enhances the heat and electron transfer capabilities of the devices, as the silver particles establish larger contact areas on both side that can absorb the heat or receive electrons at one side quicker and release the heat and electrons at the other side quicker as well.

In terms of improvements in adhesives, there are mainly studies on fillers. Wang et al. use AlN nanoparticle additive modified silver particles as fillers [39] to improve the performance of the thermal and electrical network, as well as the use of autocatalytic performance of the Cu to improve the thermal conductivity [27,28]. Ma et al. studied the silver particles sintered with different composite

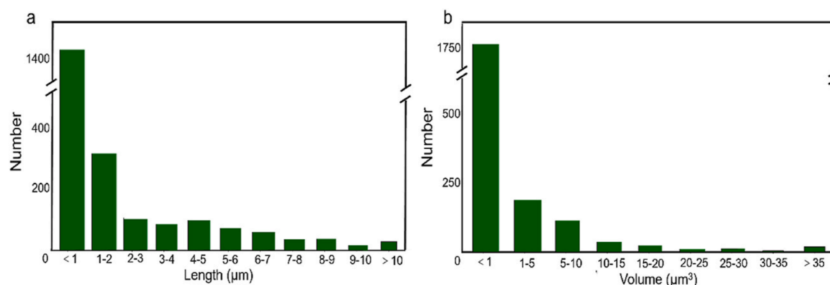

Fig. 4. Histogram of distribution of the sizes of the silver particles. (a) The length distribution of the particles. (b) The volume distribution of the particles.

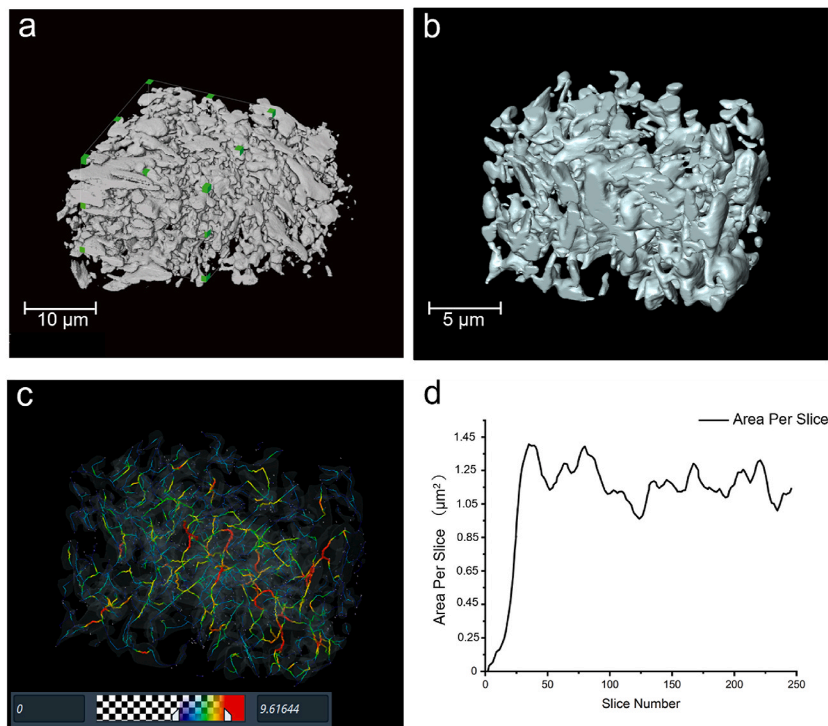

Fig. 5. 3D structural image rendering of the cropped part. (a) Cropping diagram with the green RoI box which represents the cropped part. (b) The 3D structural image of the silver particles of the cropped part. (c) The centerline network of the silver particles of the cropped part. (d) Line chart of the occupied area of the silver particles per slice (in the y direction).

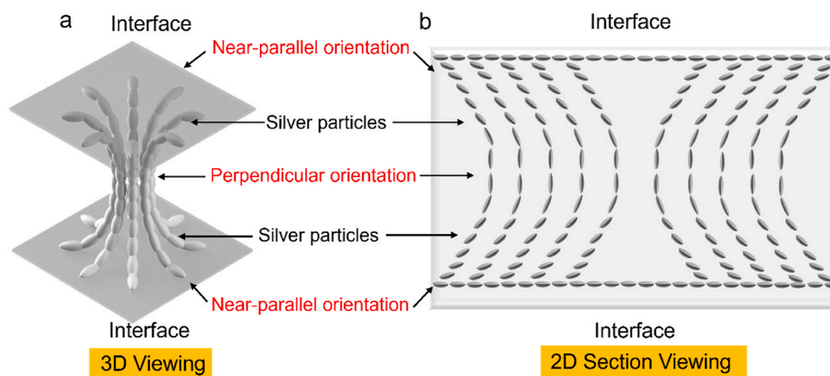

Fig. 6. Diagram of the desired internal structure of the silver epoxy adhesive. (a) 3D viewing of one of the conductive paths. (b) 2D section viewing of the structure (The grey region represents the epoxy resin matrix in the adhesive).

powders to form strong coordination bonds with silver to control the structure of the conductive filler to improve the performance [40,41]. These studies are rather costly compared with the approaches of using structural improvement only method for the (thermal) conductive network enhancement. However, the study on using structural optimization to increase the contact areas of the contact surfaces of the adhesives still very little, most of them working on increasing the number of paths between the number of contacts and contact points. In our work, the structural improvement is aimed at increasing the contact area on the (inter) surfaces and building more networks in the interior bodies to enhance the efficiency of the thermal conductivity, and hence to save the cost. At the same time, this work presented silver particles with improved sizes compared with the traditional commercially used micron-sized silver particle fillers (usually having a length of 4–55 μm and a thickness of 0.2–5 μm) [26,42], i.e. most of the silver particles here are nano-sized with a length less than 1 μm and a volume less than 1 μm^3, which is more effective in improving the thermal and electrical transfer efficiency.

4. Conclusions

X-ray nano-imaging using TXM was employed to reveal the 3D spatial structure of the conductive silver epoxy adhesive, which was proved to be an effective tool for visualizing the spatial structures of these samples containing features with heavy X-ray absorption coefficient such as silver particles. The spatial conductive path network formed by the silver particles in the adhesive was clearly visualized and analyzed. It has been found that over 60% of the silver particles are smaller than 1 μm and with a flaky shape. The results indicate that the thermal and electrical conductivity properties of this two-phase composite materials are improved by the optimized spatial arrangement of the conductive fillers: the near-perpendicular orientation of the silver particles (against the interfaces) within the inner bulk of the materials and the near-parallel orientation of these particles (against the interfaces) close to the both surfaces/ interfaces of the cured dry films. Based on these observations, a schematic proposed model of the desired internal structure of the silver epoxy adhesive is suggested. Wherein a vertically percolating silver backbone coexists with surface-parallel lattice layers at the core of the 3D network. This arrangement effectively reduces interfacial thermal resistance and electron injection barriers. The suggested model provides critical insights for designing silver epoxy adhesives with optimized conductive properties through precise control of the filler orientation and network connectivity.

CRediT authorship contribution statement

Minghao Yin: Writing – review & editing, Writing – original draft, Visualization, Validation, Software, Methodology, Investigation, Formal analysis, Data curation. **Dadong Wang:** Writing – review & editing, Writing – original draft, Validation, Resources, Investigation, Formal analysis. **Yan Zhong:** Writing – review & editing, Validation, Resources, Investigation, Formal analysis. **Ian Robinson:** Writing – review & editing, Supervision, Resources, Project administration, Methodology, Conceptualization. **Bo Chen:** Writing – review & editing, Writing – original draft, Validation, Supervision, Software, Resources, Project administration, Methodology, Investigation, Funding acquisition, Formal analysis, Data curation, Conceptualization.

Declaration of competing interest

The authors declare that they have no known competing financial interests or personal relationships that could have appeared to influence the work reported in this paper.

Acknowledgment

This work was supported by the Fundamental Research Funds for the Central Universities (Tongji University) with grant Nos. 22120210516 and 2023-2-ZD-05. The authors thank for Dr. Robert Bradley's help in carrying out the 3D X-ray tomographic experiments at the Manchester X-ray Imaging Facility (MXIF) at the University of Manchester, UK.

Data availability

Data could be available from the corresponding authors by reasonable requests.

References

[1] Y. Li, L. Shi, Y. Cheng, et al., Development of conductive materials and conductive networks for flexible force sensors, Chem. Eng. J. 455 (2023) 140763.
[2] H. Yoon, P. Matteini, B. Hwang, Review on three-dimensional ceramic filler networking composites for thermal conductive applications, J. Non-Cryst. Solids 576 (2022) 121272.
[3] J. Yan, Y. Cai, H. Zhang, et al., Rapid thermochromic and highly thermally conductive nanocomposite based on silicone rubber for temperature visualization thermal management in electronic devices, ACS Appl. Mater. Interfaces 16 (6) (2024) 7883–7893.
[4] S. Trivedi, V. Pamidi, M. Fichtner, et al., Ionically conducting inorganic binders: a paradigm shift in electrochemical energy storage, Green Chem. 24 (14) (2022) 5620–5631.
[5] P. Huang, T. Wang, Y. Zhou, et al., Piezoresistive response of MWCNTs/Epoxy mixtures with load-sensing capability, Constr. Build. Mater. 438 (2024) 137203.
[6] Z. Guo, W. Lu, Y. Zhang, et al., MXene fillers and silver flakes filled epoxy resin for new hybrid conductive adhesives, Ceram. Int. 49 (8) (2023) 12054–12060.
[7] J. Huang, W. Yang, J. Zhu, et al., Silver nanoparticles decorated 3D reduced graphene oxides as hybrid filler for enhancing thermal conductivity of polystyrene composites, Compos. Appl. Sci. Manuf. 123 (2019) 79–85.
[8] H. Niu, H. Guo, L. Kang, et al., Highly thermally conductive and soft thermal interface materials based on vertically oriented boron nitride film, Compos. B Eng. 272 (2024) 111219.
[9] G. Cao, S. Cai, H. Zhang, et al., The mixture of silver nanowires and nanosilver-coated copper micronflakes for electrically conductive adhesives to achieve high electrical conductivity with low percolation threshold, Adv. Compos. Hybrid Mater. 5 (3) (2022) 1730–1742.
[10] Z. Zheng, X. Lu, L. Xu, et al., Constructing phonon transport bridges via low-temperature sintering in Diamond@ Ag/EP composite to achieve efficient 3D networks structure, Chem. Eng. J. 495 (2024) 153499.
[11] D. Wang, H. Wei, Y. Lin, et al., Achieving ultrahigh thermal conductivity in Ag/MXene/epoxy nanocomposites via filler-filler interface engineering, Compos. Sci. Technol. 213 (2021) 108953.
[12] Y. Chen, X. Hou, M. Liao, et al., Constructing a "pea-pod-like" alumina-graphene binary architecture for enhancing thermal conductivity of epoxy composite, Chem. Eng. J. 381 (2020) 122690.
[13] D. Ma, A. Arora, S. Deng, et al., Quantifying phonon particle and wave transport in silicon nanophononic metamaterial with cross junction, Mater. Today Phy. 8 (2019) 56–61.
[14] Y. Zhao, X. Zeng, L. Ren, et al., Heat conduction of electrons and phonons in thermal interface materials, Mater. Chem. Front. 5 (15) (2021) 5617–5638.
[15] Y.X. Zhang, Q.Y. Huang, X. Yan, et al., Synergistically optimized electron and phonon transport in high-performance copper sulfides thermoelectric materials via one-pot modulation, Nat. Commun. 15 (1) (2024) 2736.

[16] X.X. He, D. Ou, S.Y. Wu, et al., A mini review on factors affecting network in thermally enhanced polymer composites: filler content, shape, size, and tailoring methods, Adv. Compos. Hybrid Mater. 5 (1) (2022) 21–38.
[17] C. Wang, Y. Gong, B.V. Cunning, et al., A general approach to composites containing nonmetallic fillers and liquid gallium, Sci. Adv. 7 (1) (2021) 3767.
[18] H. Li, C. Fu, N. Chen, et al., Ice-templated assembly strategy to construct three-dimensional thermally conductive networks of BN nanosheets and silver nanowires in polymer composites, Compos. Commun. 25 (2021) 100601.
[19] L. Shubhadarshinee, P. Mohapatra, B.R. Jali, et al., Synthesis and characterization of a novel silver nanoparticles decorated functionalized single-walled carbon nanotubes nanohybrids embedded polyaniline ternary nanocomposites: thermal, dielectric, and sensing properties, Polymer-Plastics Technol. Mater. 62 (2) (2023) 197–217.
[20] R. Kumar, A. Mishra, S. Sahoo, et al., Epoxy-based composite adhesives: effect of hybrid fillers on thermal conductivity, rheology, and lap shear strength, Polym. Adv. Technol. 30 (6) (2019) 1365–1374.
[21] M. Zulkarnain, M.A. Fadzil, M. Mariatti, et al., Effects of silver microparticles and nanoparticles on thermal and electrical characteristics of electrically conductive adhesives, J. Electron. Mater. 46 (2017) 6727–6735.
[22] Y. Chen, Q. Li, C. Li, et al., Regulation of multidimensional silver nanostructures for high-performance composite conductive adhesives, Compos. Appl. Sci. Manuf. 137 (2020) 106025.
[23] J. Li, N. Li, X. Wan, et al., Synthesis of monodispersed plate-shaped silver particles: with high tap-density and low radius-thickness ratio, J. Mater. Res. Technol. 19 (2022) 2497–2509.
[24] X. Li, X. Xiang, L. Wang, et al., Conductivity and mechanical properties of conductive adhesive with silver nanowires, Rare Met. 37 (2016) 191–195.
[25] W. Zhang, J. Wang, H. Liu, et al., Surface treatment of micron silver flakes with coupling agents for high-performance electrically conductive adhesives, Int. J. Adhesion Adhes. 122 (2023) 103300.
[26] Y. Lai, S. Zhu, J. Li, et al., One-step synthesis of micro-sized flake silver particles as electrically conductive adhesive fillers in printed electronics, J. Ind. Eng. Chem. 121 (2023) 77–91.
[27] Z. Sun, N. Cheng, F. Chen, et al., Preparation of micron-scale Cu@ Ag conductive particles by displacement coating to reinforce epoxy conductive adhesives, New J. Chem. 45 (22) (2021) 10089–10097.
[28] H. Fang, C. Wang, S. Zhou, et al., Rapid pressureless and low-temperature bonding of large-area power chips by sintering two-step activated Ag paste, J. Mater. Sci. Mater. Electron. 31 (2020) 6497–6505.
[29] C. Li, Q. Li, L. Cheng, et al., Conductivity enhancement of polymer composites using high-temperature short-time treated silver fillers, Compos. Appl. Sci. Manuf. 100 (2017) 64–70.
[30] Z. Chen, M. Zhang, P. Ren, et al., Enhanced mechanical and tribological properties of epoxy composites reinforced by novel hyperbranched polysiloxane functionalized graphene/MXene hybrid, Chem. Eng. J. 466 (2023) 143086.
[31] Z. Sun, J. Li, M. Yu, et al., A review of the thermal conductivity of silver-epoxy nanocomposites as encapsulation material for packaging applications, Chem. Eng. J. 446 (2022) 137319.
[32] F. Chen, H. Xiao, Z.Q. Peng, et al., Thermally conductive glass fiber reinforced epoxy composites with intrinsic self-healing capability, Adv. Compos. Hybrid Mater. 4 (2021) 1048–1058.
[33] M. Mazaheri, J. Payandehpeyman, M. Khamehchi, A developed theoretical model for effective electrical conductivity and percolation behavior of polymer-graphene nanocomposites with various exfoliated filleted nanoplatelets, Carbon 169 (2020) 264–275.
[34] S.H. Ji, D. Lee, J.S. Yun, Experimental and theoretical investigations of the rheological and electrical behavior of nanocomposites with universal percolation networks, Compos. B Eng. 225 (2021) 109317.
[35] L. Ye, D. Qiu, L. Peng, et al., Microstructures and electrical conductivity properties of compressed gas diffusion layers using X-ray tomography, Appl. Energy 326 (2022) 119934.
[36] J.T. Lang, D. Kulkarni, C.W. Foster, et al., X-Ray tomography applied to electrochemical devices and electrocatalysis, Chem. Rev. 123 (16) (2023) 9880–9914.
[37] M. Feng, Y. Pan, M. Zhang, et al., Largely improved thermal conductivity of HDPE composites by building a 3D hybrid fillers network, Compos. Sci. Technol. 206 (2021) 108666.
[38] S. Jasmee, G. Omar, S.S.C. Othaman, et al., Interface thermal resistance and thermal conductivity of polymer composites at different types, shapes, and sizes of fillers: a review, Polym. Compos. 42 (6) (2021) 2629–2652.
[39] J. Wang, S. Yodo, H. Tatsumi, et al., Thermal conductivity and reliability reinforcement for sintered microscale Ag particle with AlN nanoparticles additive, Mater. Char. 203 (2023) 113150.
[40] P. Maroulas, D. Dragatogiannis, A. Kyritsis, et al., Electrical/thermal conductivities of low-temperature sintered/Ag-decorated epoxy microspheres, Mater. Chem. Phys. 319 (2024) 129355.
[41] L. Ma, Y. Wang, Q. Jia, et al., Low-temperature-sintered nano-Ag film for power electronics packaging, J. Electron. Mater. 53 (1) (2024) 228–237.
[42] N. Li, J. Li, X. Wan, et al., Preparation of micro-size spherical silver particles and their application in conductive silver paste, Materials 16 (4) (2023) 1733.